

# Osmotic pressure of compressed lattice knots

EJ Janse van Rensburg<sup>1</sup>

<sup>1</sup>*Department of Mathematics & Statistics, York University, Toronto, ON, Canada, M3J 1P3*

(Dated: April 25, 2019)

A numerical simulation shows that the osmotic pressure of compressed lattice knots is a function of knot type, and so of entanglements. The osmotic pressure for the unknot goes through a negative minimum at low concentrations, but in the case of non-trivial knot types  $3_1$  and  $4_1$  it is negative for low concentrations. At high concentrations the osmotic pressure is divergent, as predicted by Flory-Huggins theory. The numerical results show that each knot type has an equilibrium length where the osmotic pressure for monomers to migrate into or out of the lattice knot is zero. Moreover, the lattice unknot is found to have two equilibria, one unstable, and one stable, whereas the lattice knots of type  $3_1$  and  $4_1$  have one stable equilibrium each.

PACS numbers: 36.20.-r, 61.25.Hq, 82.35.-x, 87.15.-v

## COMPRESSED LATTICE KNOTS

Confinement of a biopolymer (eg. in an organelle in a living cell) causes an increase in knotting (and so in topological entanglement) [33]. The confinement compresses the biopolymer and this is known to increase self-entanglements in the backbone of the polymer [39]. It is known that entanglements have an effect on the physical properties of biopolymer such as DNA [9]. Topological entanglement (knotting and linking) also impedes the movement of DNA, for example in the ejection of DNA from a viral capsid [31] or the speed of electrophoretic migration of polymers [42].

The genome of prokaryotes (bacteria) is a circular double helix DNA molecule compressed in a small volume (as opposed to the volume occupied by free DNA in a good solvent) [6]. Cellular processes replicating and transcribing DNA involves the unwinding and recombination of DNA, and errors in these processes may result in the loss or addition of base pairs (that is, in mutations by insertion or deletion of basepairs in the genome; these are point mutations [7], and see for example references [5] and [30]). The fidelity or accuracy of DNA replication and transcription processes is driven by free energy gradients due to binding energies and conformational and translational degrees of freedom. The tendency to insert or lose base-pairs (that is, of point mutations occurring) from the DNA backbone can be modelled as an osmotic pressure of the base-pairs bound in the backbone. If this pressure is positive, then base-pairs could escape when their local environment is disrupted by topoisomerases or other enzymes driving replication or transcription. If it is negative, then base-pairs in solution will tend to be added in these processes. A large osmotic pressure in either direction will tend to degrade the fidelity of replication and transcription processes.

Since circular DNA molecules are in confining environments in a cell, the osmotic pressure of basepairs can be

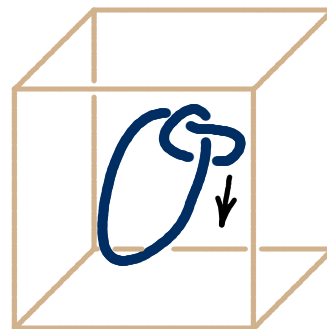


FIG. 1: A model of a knotted ring polymer in a cavity. Contributions to the entropy are due to translational degrees of freedom, topological constraints due to the knot, and conformational degrees of freedom.

modelled by placing a closed random string [14–16, 18] in a confining space (see Fig. 1). The entropy of the random string can be quantified by placing it in a lattice. If it is self-avoiding, then it is a closed self-avoiding walk [18, 19, 22] and this is a lattice model of a ring polymer in a good solvent. A closed self-avoiding walk is a *lattice polygon* [12, 20, 23].

Lattice polygons are knotted asymptotically with probability 1 [35, 40]. A lattice polygon with fixed knot type is a *lattice knot* [11, 13]. It is known that the entropy of a lattice knot is a function of its knot type [29, 34]. *Tight lattice knots* [11] are minimal length lattice knots [24, 26, 37]. The compressibility of tight lattice knots is known to be a function of knot type [21, 28].

In Fig. 2 the model in Fig. 1 is quantified by placing and compressing a lattice knot in a cubical box (this is a lattice version with self-avoidance of the model in reference [3]). The entropy of the *compressed lattice knot* has contributions from translational degrees of freedom (if it is small compared to the side length of the box), from topological constraints (due to entanglements which depends on the knot type), and from conformational de-

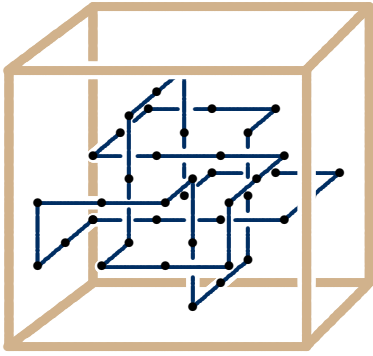


FIG. 2: A lattice knot in a cubical cavity.

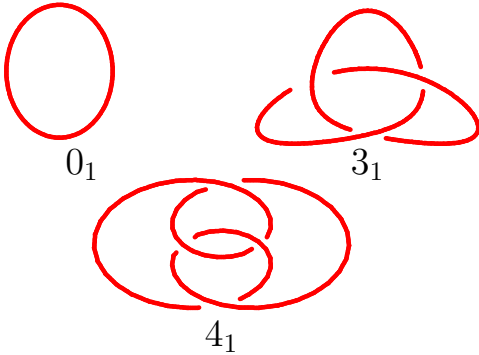


FIG. 3: The unknot  $0_1$ , the trefoil knot  $3_1$  and the figure eight knot  $4_1$  [1, 36].

degrees of freedom. In this paper compressed lattice knots of three knot types [1, 36], namely the *unknot* ( $0_1$ ), the *trefoil* ( $3_1$ ), and the *figure eight knot* ( $4_1$ ) will be considered; see Fig. 3.

A cube in the lattice of side-length  $L-1$  has volume  $V = L^3$  and side-length  $L$ . The maximum length of a lattice knot confined to a cube of side-length  $L$  is  $L^3$  if  $L$  is even, and  $L^3-1$  if  $L$  is odd. The *lattice unknot* has minimal length 4 and there are  $3L(L-1)^2$  ways it can be placed in the cube. The *lattice trefoil knot*  $3_1$  can be tied with 24 steps in the cubic lattice [13], and there are 3328 conformations distinct under translations in the cubic lattice [38]. None of these tight lattice trefoils can be realised in a cube of side-length 3, but a numerical simulation detected 4168 distinct placements of 3304 tight lattice trefoils in a cube of side-length 4, and 30104 distinct placements of tight lattice trefoils in a cube of side-length 5. Similarly, a *tight lattice figure eight knot*  $4_1$  has minimal length 30 in the cubic lattice [38] and there are 3648 conformations distinct under translations in the cubic lattice. A computer count shows that none of these can be realised in a cube of side-length 3, but there are 864 distinct placements of tight lattice figure eight knots in a cube of side-length 4, and 18048 distinct placements in a cube of side-length 5.

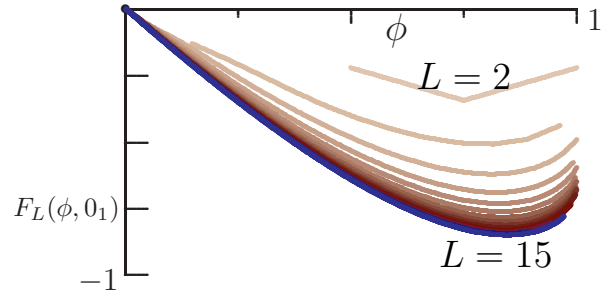


FIG. 4: The free energy per unit volume for unknotted lattice knots, for  $2 \leq L \leq 15$ .

## FREE ENERGY AND OSMOTIC PRESSURE

Denote the number of distinct placements of lattice knots of length  $n$ , of knot type  $K$ , confined in a cube of side-length  $L$ , by  $p_{n,L}(K)$ . Then, for example,  $p_{24,3}(3_1) = 0$  and  $p_{24,4}(3_1) = 4168$ . Approximate enumeration of  $p_{n,L}(K)$  can be done by using the GAS algorithm [25] implemented with BFACF moves [2, 4]. See reference [27] for details.

The concentration of vertices in a lattice knot in a cube of side-length  $L$  is  $\phi = \frac{n}{V}$  where  $V = L^3$ . The free energy at concentration  $\phi$  of lattice knots of type  $K$  is

$$F_{tot}(\phi; K) = -\log p_{n,L}(K), \quad (1)$$

where  $n = \phi V$ . The free energy per unit volume is  $F_L(\phi; K) = \frac{1}{V} F_{tot}(\phi; K)$  and this is plotted in Fig. 4 for  $2 \leq L \leq 15$  and for  $K = 0_1$  (the unknot) against the monomer concentration  $\phi$ . The shape of these curves is consistent with prediction of Flory-Huggins theory [10].

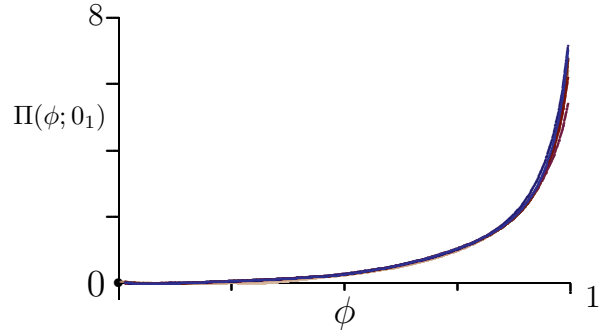


FIG. 5: The calculated osmotic pressure of compressed lattice unknots. The data are for  $2 \leq L \leq 15$ .

The osmotic pressure  $\Pi(\phi; K)$  of compressed lattice knots is given by

$$\Pi(\phi; K) = -\frac{d}{dV} F_{tot}(\phi; K). \quad (2)$$

Changing variables to  $\phi$  shows that

$$\Pi(\phi; K) = \phi^2 \frac{d}{d\phi} \left( \frac{1}{\phi} F_L(\phi; K) \right) \quad (3)$$

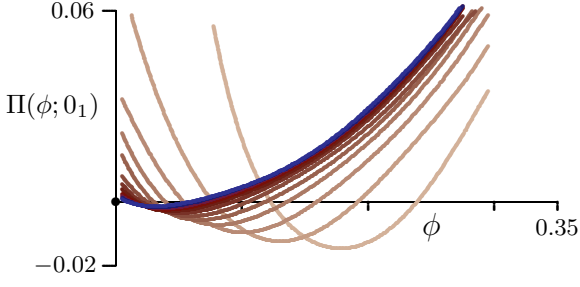


FIG. 6: The osmotic pressure of compressed lattice unknots at low concentration for  $3 \leq L \leq 15$ .

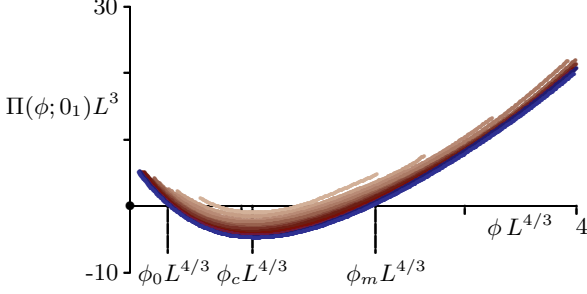


FIG. 7: Rescaled osmotic pressures for the unknot  $0_1$ , plotted as a function of  $\phi L^{4/3}$ . The data are for  $3 \leq L \leq 15$ .

in terms of the free energy per unit volume. This can be computed from the data in figure 4 by taking a numerical derivative. Using a central second order numerical approximation to the derivative gives Fig. 5. This appears to be consistent with the predicted Flory-Huggins osmotic pressure:  $\Pi(\phi; 0_1)$  is increasing and sharply diverges as  $\phi \rightarrow 1^-$ . Closer examination of Fig. 5 shows that  $\Pi(\phi; 0_1)$  is not monotone but is decreasing at low concentrations and negative and not monotonic on an interval of low concentrations; see Fig. 6.

At negative osmotic pressure the lattice unknot will add length. Similarly, at positive osmotic pressure the lattice unknot will shed length and become smaller. The pressure curves in Fig. 6 are functions of  $L$  and each has two zeros at  $\phi_0$  and  $\phi_m$ . At concentrations  $\phi < \phi_0$  the lattice unknot will evaporate, and when  $\phi_0 < \phi < \phi_m$  it will add length until the concentration is  $\phi_m$  (which is a stable fixed point). It will also shed length if  $\phi > \phi_m$  until the concentration is  $\phi_m$ .

Lattice polygons of length  $n$  has linear size  $O(n^\nu)$  where  $\nu \approx \frac{3}{5}$  is the metric exponent in three dimensions [19] (a more accurate estimate is  $\nu \approx 0.587597(7)$  [8]). Effects of the confining cube will become important when  $n^\nu \sim L$ . The osmotic pressure should vanish at this point; the result is that  $\phi_m \sim L^{1/\nu}/L^3 = L^{1/\nu-3}$ . As  $\phi \rightarrow 0^+$ ,  $\Pi(\phi; K) \sim L^{-3}$ . Using the Flory value for  $\nu$  and then plotting  $\Pi(\phi; K)L^3$  as a function of  $\phi L^{4/3} \approx \phi L^{4/3}$  should collapse the data in Fig. 6. This is shown in Fig. 7, although there are still finite size corrections. Extrapolating the zeros of the curves in

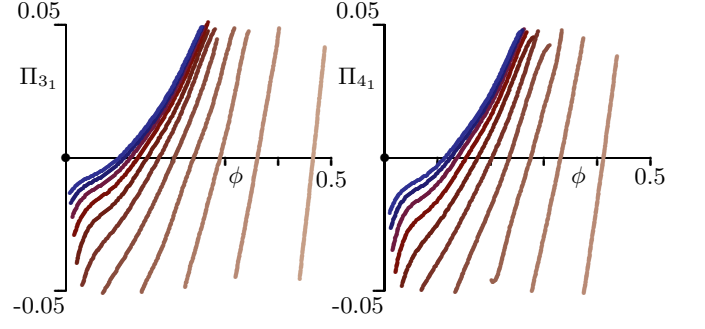


FIG. 8: The osmotic pressure  $\Pi_{3_1} \equiv \Pi(\phi; 3_1)$  of the trefoil knot, and  $\Pi_{4_1} \equiv \Pi(\phi; 4_1)$  of the figure eight knot plotted against the concentration  $\phi$  for  $0 \leq \phi \leq 0.5$ .

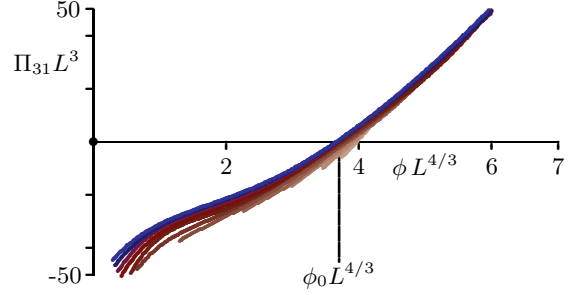


FIG. 9: Rescaled osmotic pressures  $\Pi_{3_1} \equiv \Pi(\phi; 3_1)$  for lattice knots of type  $3_1$  (trefoil). The data are taken from the left panel in Fig. 8 for  $4 \leq L \leq 15$ .

Fig. 7 gives  $\phi_0 \simeq 0.149 L^{-4/3}$ ,  $\phi_m \simeq 0.286 L^{-4/3}$ . Since the osmotic pressure vanishes at these concentrations the equilibrium lengths at which the osmotic pressure vanishes are  $n_0 \simeq 0.149 L^{5/3}$  and  $n_m \simeq 0.286 L^{5/3}$ . The osmotic pressure of the unknot goes through a minimum at  $\phi_c \simeq 0.209 L^{-4/3}$ .

The osmotic pressures of compressed lattice knots at low concentration and of knot types  $3_1$  and  $4_1$  are plotted in Fig. 8. Here the osmotic pressures are monotone increasing with concentration  $\phi$ , passing through zero at a critical concentration  $\phi_0$ . Rescaling the data in the same way as in Fig. 7 gives Figs. 9 and 10. This shows that for  $3_1$ ,  $\phi_0 L^{4/3} \simeq 3.94 L^{-4/3}$ , and for  $4_1$ ,

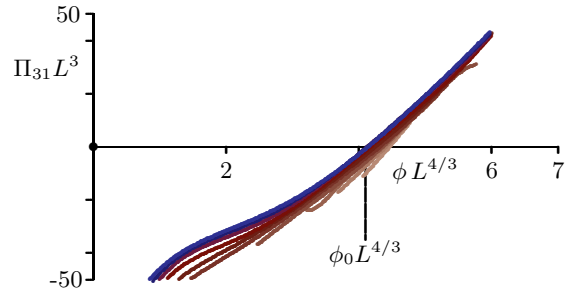


FIG. 10: Rescaled osmotic pressures  $\Pi_{4_1} \equiv \Pi(\phi; 4_1)$  for lattice knots of type  $4_1$  (figure eight knot). The data are taken from the right panel in Fig. 8 for  $4 \leq L \leq 15$ .

$\phi_0 L^{4/3} \simeq 4.48 L^{-4/3}$ . For  $\phi < \phi_0$  the osmotic pressure is negative and the lattice knot will grow to an equilibrium length  $n_0 \simeq 3.94 L^{5/3}$  for  $3_1$  and  $n_0 \simeq 4.48 L^{5/3}$  for  $4_1$ .

## CONCLUSION

In this letter a numerical simulation of compressed lattice knots as a model of an entangled ring polymer show that the osmotic pressure is a function of knot type. Since the level of entanglements is a function of knot type, these results support the notion that the properties of confined biopolymers, such as DNA, is a function of the level of entanglement if the biopolymer is confined or compressed in a narrow space, or adsorbed on a membrane. Adsorption of the knotted polymer on the surface of a membrane was analysed in the lattice in reference [41]. If the polymer can relax freely after adsorption, then the knot localizes and its effects disappear as the length of the polymer increases [17, 32]. On the other hand, the adsorbed polymer should have properties of projected three dimensional polymers; experimental evidence of this was given in reference [17].

The numerical data in this paper show that the rescaled osmotic pressure vanishes at a critical concentrations, as shown in Figs. 7, 9 and 10, and that these critical concentrations are functions of knot types. In the case of the unknot there are two critical concentrations where the osmotic pressure vanishes. At these concentrations the lattice unknot has an equilibrium length, but at the lower critical concentration this is unstable, and the unknot will tend to grow or evaporate. At the higher critical concentration the equilibrium length is stable. The situation is not the same for the trefoil and figure eight knot types. In these cases there is one stable equilibrium at a critical concentration which is dependent on knot type.

## Acknowledgements

EJJvR acknowledges support from NSERC(Canada) in the form of Discovery Grant RGPIN-2014-04731.

- 
- [1] C.C. Adams, *The knot book: An elementary introduction to the mathematical theory of knots*, AMS (2004).
  - [2] C. Aragao de Carvalho, S. Caracciolo & J. Fröhlich, Nucl. Phys. B **215**, 209 (1983).
  - [3] J. Arsuaga *et al.*, PNAS **102**(26), 9165 (2005).
  - [4] B. Berg & D. Foerster, Phys. Lett. B **106**, 323 (1981).
  - [5] D.E. Berg, A. Weiss & L. Crossland, J Bact. **142**(2), 439 (1980).

- [6] J. Cairns, Cold Springs Harbor Symp. on Quant. Bio. **28**, 43 (1963).
- [7] S. Clancy, Nature Education **1**(1), 187 (2008).
- [8] N. Clisby, Phys. Rev. Lett. **104**, 055702 (2010).
- [9] N. Cozzarelli, Proc. Symp. Appl. Math. **45**, 1 (1992)
- [10] P-G. de Gennes, *Scaling Concepts in Polymer Physics*, Cornell (1979).
- [11] P-G. de Gennes, Macromol. **17**, 703 (1984).
- [12] M. Delbrück, Proc. Symp. Appl. Math. **14**, 55 (1962).
- [13] Y. Diao, J. Knot Theo. Ram. **2**, 413 (1993).
- [14] S.F. Edwards, Proc. Phys. Soc. **85**, 613 (1965).
- [15] S.F. Edwards, Proc. Phys. Soc. **91**, 513 (1967).
- [16] S.F. Edwards, J. Phys. A: Gen. Phys. **1**, 15 (1968).
- [17] E. Ercolini *et al.*, Phys. Rev. Lett. **98**, 058102 (2007).
- [18] P.J. Flory, Proc. Roy. Soc. London Ser. A. **234**, 60 (1956).
- [19] P.J. Flory, *Statistical Mechanics of Chain Molecules*, Interscience (1969).
- [20] H.L. Frisch & E. Wasserman, J. Amer. Chem. Soc. **83**, 3789 (1961).
- [21] D. Gasumova *et al.*, J. Stat. Mech: Theo. Expr. **P09004** (2012).
- [22] J.M. Hammersley, Proc. Camb. Phil. Soc. **53**, 642 (1957).
- [23] J.M. Hammersley, Proc. Camb. Phil. Soc. **57**, 516 (1961).
- [24] E.J. Janse van Rensburg & S.D. Promislow, J. Knot. Theor. Ram. **4**(1) 115 (1995).
- [25] E.J. Janse van Rensburg & A. Rechnitzer, J. Phys. A: Math. Theor. **42** 335001 (2009).
- [26] E.J. Janse van Rensburg & A. Rechnitzer, J. Stat. Mech: Theo. Expr. **P09008** (2011).
- [27] E.J. Janse van Rensburg & A. Rechnitzer, J. Knot. Theor. Ram. **20**, 1145 (2011).
- [28] E.J. Janse van Rensburg & A. Rechnitzer, J. Stat. Mech: Theo. Expr. **P05003** (2012).
- [29] E.J. Janse van Rensburg, J. Stat. Mech: Theo. Expr. **P06017** (2014).
- [30] T.A. Kunkel & K. Bebenek, Ann. Rev. Biochem. **69**, 497 (2000).
- [31] D. Marenduzzo, C. Micheletti, E. Orlandini & D.W. Sumners, Proc. Natl. Acad. Sci. **110**(50), 20081 (2013).
- [32] R. Metzler *et al.*, Phys. Rev. Lett. **88**, 188101 (2002).
- [33] E. Orlandini & C. Micheletti, J. Biol. Phys. **39**, 267 (2013).
- [34] E. Orlandini *et al.*, J. Phys. A: Math. Gen. **31**, 5953 (1998).
- [35] N. Pippenger, Disc. Appl. Math. **25**, 273 (1989).
- [36] D. Rolfsen, *Knots and Links*, American Mathematical Society (2003).
- [37] R. Scharein *et al.*, J. Phys. A: Math. Theor. **42**, 475006 (2009).
- [38] R. Scharein *et al.*, J. Phys. A: Math. Theor. **45**, 065003 (2012).
- [39] J. Tang, N. Du & P.S. Doyle, Proc. Natl. Acad. Sci. **108**(39), 16153 (2011).
- [40] D.W. Sumners & S.G. Whittington, J. Phys. A: Math. Gen. **21**, 1689 (1988).
- [41] C. Vanderzande, J. Phys. A: Math. Gen. **28**, 3681 (1995).
- [42] C. Weber *et al.*, Biophys J. **90**(9), 3100 (2006).